

Ablation of C/SiC, C/SiC–ZrO₂ and C/SiC–ZrB₂ composites in dry air and air mixed with water vapor

Xufei Fang^a, Fangsheng Liu^a, Hengqiang Su^a, Bin Liu^b, Xue Feng^{a,*}

^aAML, Department of Engineering Mechanics, Tsinghua University, Beijing 100084, China

^bAerospace Research Institute of Special Material and Process Technology, Beijing 100074, China

Received 31 August 2013; received in revised form 1 October 2013; accepted 1 October 2013

Available online 12 October 2013

Abstract

C/SiC composites with different additives (ZrO₂ and ZrB₂) were fabricated by CVI and CVD and their oxidation and ablation properties at 1700–1800 °C were investigated. Two different ablation test conditions, dry air and air mixed with water vapor, are compared. The ablation test results are reviewed, the weight loss rates are presented and the corresponding micro-structures are investigated in detail. The results show that in dry air, the weight loss rate of C/SiC composites is greater than those with ZrO₂ and ZrB₂ additives. However, in air mixed with water vapor (5 wt%) to simulate the hygrothermal condition, the weight loss rates of these three composites all become relatively smaller. A model is proposed to predict the weight loss of C/SiC composites and it agrees well with the experimental data.

© 2013 Elsevier Ltd and Techna Group S.r.l. All rights reserved.

Keywords: C/SiC composites; Ablation; Water vapor

1. Introduction

C/SiC composites have been attracting increasing interest in recent years due to their unique properties at high temperatures. They have been widely used in the leading edges of airfoils, thermal protection systems and aeronautic engines [1–6]. They possess an outstanding oxidation resistance because of the formation of a silica layer [7–9]. However, at ultra-high temperatures above 1600 °C, the oxidation resistance degrades due to the onset of active oxidation of the silica layer [10,11] and the stress-oxidation coupling effect that follows [12]. In order to improve the ablation and oxidation resistance of the C/SiC composites at ultra-high temperatures, a potentially effective approach is to introduce ultra-high temperature ceramics (UHTCs) such as ZrB₂ into the substrate of the composites. UHTCs have very high melting points, above 3000 °C, and outstanding mechanical properties such as high hardness and strength [13,14]. Structural components made from these materials have many potential applications

due to their excellent properties at high temperature, such as superior ablation/oxidation resistance and good thermal-shock resistance [15–20]. There have already been some studies introducing UHTCs particles into C/SiC composites and the high-temperature performance of these composites have also been studied [21–24]. However, still, with longer application, especially in combustion chambers, after the anti-oxidation coatings are destroyed, the substrate of the materials becomes exposed to the complicated combustion environment and becomes vulnerable to the water vapor and inorganic salts, which would cause severe erosion and damage to the components. Thus, it is of great importance to study the behavior of the materials under the working conditions and evaluate the oxidation and ablation properties of and corresponding mechanisms in order to discover ways to improve the properties of these composites.

In this work, we present the results of the ablation behavior of C/SiC composites with different additives (ZrO₂ and ZrB₂) at 1700–1800 °C for 600 s in dry air and with water vapor. In order to further predict and evaluate the weight loss rate of such materials, a primary numerical model of the ablation process is developed. This finding may provide a fundamental understanding of the ablation properties of the materials under working conditions.

*Corresponding author. Tel./fax: +86 10 62 781 465.

E-mail addresses: fengxue@tsinghua.edu.cn,
xfeng9@gmail.com (X. Feng).

2. Experimental procedure

2.1. Preparation of the composites

The composites were fabricated using a 3-stage process. Firstly, chemical vapor deposition (CVD) was used to prepare a layer of pyrolytic carbon (PyC) fiber on the surface of the pre-forms as the interface phase. Then the treated pre-forms were put through a densification process by chemical vapor infiltration (CVI). In the third step, the CVD technique was used again to deposit SiC coatings on the surface of the specimens for the purpose of preventing oxidation. The size of the prepared samples used in the experiment was 30 mm × 30 mm × 10 mm. In order to investigate the different properties of the C/SiC composites, different additives were used in the composite. We developed three types of composites, namely; C/SiC, C/SiC–ZrO₂ (15 wt%) and C/SiC–ZrB₂ (15 wt%) by introducing ZrO₂ and ZrB₂ micro-powders into the pre-forms.

2.2. Ablation test and characterization

The specimens were ablated vertically with an oxyacetylene torch flame. The inner diameter of the nozzle tip was 2 mm. The distance between the nozzle tip and specimen surface was 10 mm. The pressure and flux of oxygen were 0.45 MPa and 4.14 L/min, and 0.09 MPa and 2.46 L/min for acetylene. Experiments in dry air and air/water vapor mix (5 wt% vapor) were carried out for the three different types of specimens, C/SiC, C/SiC–ZrO₂ and C/SiC–ZrB₂. The ablation time was 600 s. Fig. 1 shows a schematic of the experimental set-up with two infrared laser temperature detectors for measuring the surface temperature and a high speed camera (Redlake-X3) for recording the real-time surface changes. The morphology and the

fracture surfaces of the composites were inspected with a scanning electron microscope (SEM, Zeiss-Supra 55) after the tests.

3. Results and analysis

For each type of composite and test condition, three samples were tested, and the average weight loss rates were calculated, as presented below. It should be noted that there was very little material washed away directly off the specimen during the process of heating and cooling as observed in the experiments, thus we ignored the influence of the weight loss during heating and cooling process when we calculated the weight loss rate for all the specimens.

3.1. Results and analysis in dry air

The ablation test conditions and results for the specimens in dry air are listed in As can be seen from Table 1, in dry air the weight loss rate of C/SiC is highest, while the weight loss rates of C/SiC–ZrO₂ and C/SiC–ZrB₂ are almost the same. Firstly, compared with the oxidation product SiO₂ from SiC, the oxidation product ZrO₂ from composites C/SiC–ZrO₂ and C/SiC–ZrB₂ possesses a lower saturated vapor pressure and a higher heat of solution (SiO₂, 8.82 kJ/mol; ZrO₂, 215.4 kJ/mol), making it more difficult for ZrO₂ to volatilize [25]. Secondly, the SiC improves the oxidation resistance of ZrB₂ and ZrO₂, due

Table 1
Ablation test conditions and results for the specimens in dry air.

Types	C/SiC	C/SiC–ZrO ₂	C/SiC–ZrB ₂
Weight loss rate (mg/s)	2.05	1.90	1.91
Ablation time (s)	600	600	600
Average temperature (°C)	1760	1756	1757

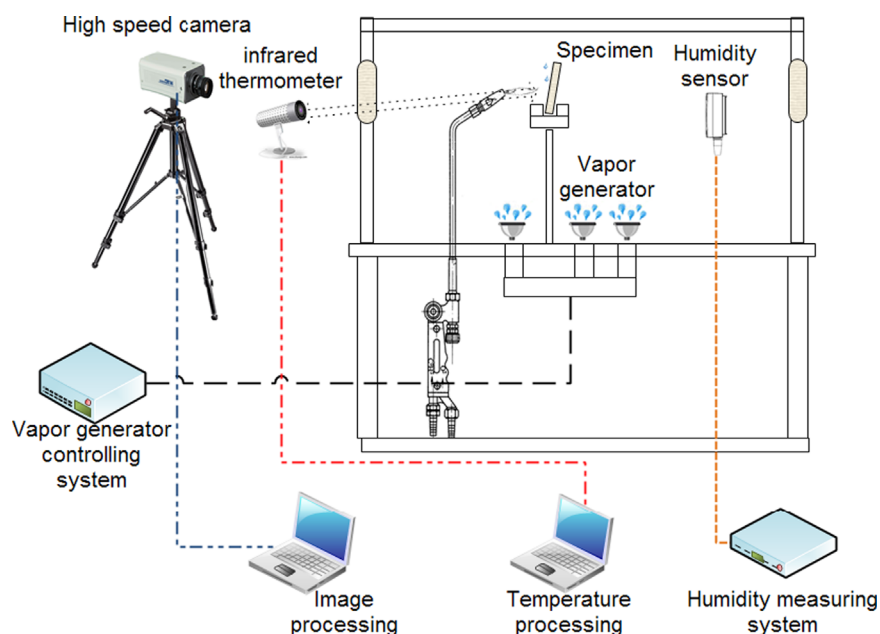


Fig. 1. Scheme of the apparatus for ablation simulation with water vapor.

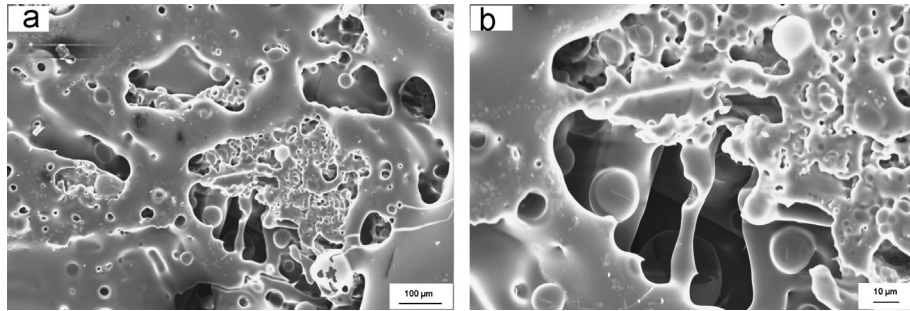


Fig. 2. Typical ablation morphologies of specimen C/SiC in dry air (a) center of ablation pit, and (b) magnified ablation pit.

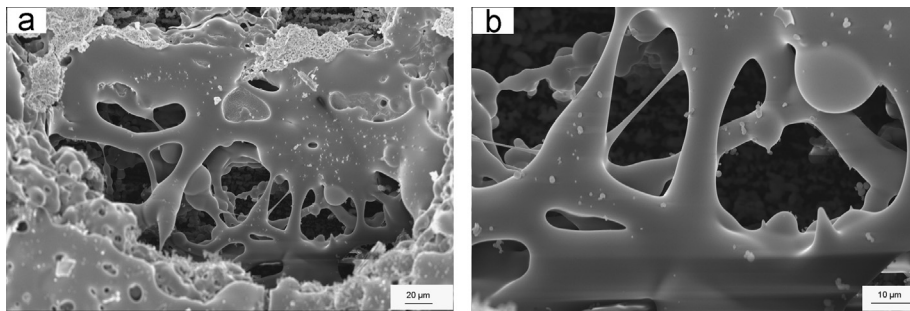


Fig. 3. Typical ablation morphologies of specimen C/SiC–ZrO₂ in dry air (a) center of ablation pit, and (b) magnified ablation pit.

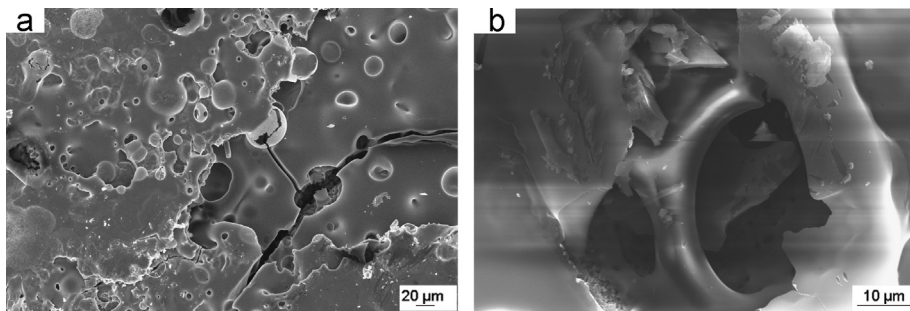


Fig. 4. Typical ablation morphologies of specimen C/SiC–ZrB₂ in dry air (a) center of ablation pit, and (b) magnified ablation pit.

to the formation of a protective SiO₂-glassy layer which prevents oxygen penetration in the bulk of the material [26]. Thirdly, the morphology of the oxidized scale consists of an outermost glassy layer of borosilicate [27], forming a glassy layer of ZrSiO₄ when used in oxidative atmosphere [28,29]. For the above reasons, a mutually reinforcing effect is created against ablation and oxidation between the substrate (C/SiC) and the additives (ZrO₂ and ZrB₂), which leads to improved ablation resistance of C/SiC–ZrO₂ and C/SiC–ZrB₂ compared to that of C/SiC.

Furthermore, the SEM morphologies in Figs. 2–4 show that in dry air, the anti-oxidation coatings of the three types of composites were all destroyed and there were “bone structures” in the ablation pits.

The ablation process was captured with a high speed camera (with filters on the lens). The liquid oxides generated were washed away to the outside of the ablation core, forming a protective layer.

Specifically, the melting point of SiO₂ is within the range of 1670–1710 °C, while that of B₂O₃ is about 445 °C, and the boiling point of B₂O₃ is 1500 °C. When heated to 600 °C, B₂O₃ becomes a highly viscous liquid. So under the conditions of the experiment, the B₂O₃ volatilized, while most of the liquid SiO₂ remained on the surface and solidified around the ablation pit where the temperature was lower than the ablation core (lower than melting point of SiO₂). But since the melting point of ZrO₂ is around 2700 °C, the reaction product ZrO₂ mainly remained on the surface, forming a protective oxide layer around the center of the ablation pit.

The bubbling effect of the liquid SiO₂ as the temperature exceeded its melting point was also captured with the high speed camera. For the “bone structures” mentioned above, the formation of the typical structure is due to the viscosity of the liquid SiO₂, as within the temperature range of our experiment (which is around the melting point of SiO₂), the liquid SiO₂ formed this structure as it solidified when the temperature

decreased. Similarly, around the center of the ablation pit, as the ablation temperature decreased and the speed of the gas declined, a layer of solid glassy oxide (mainly SiO_2 and ZrO_2) built up, which further covered the cracks and prevented the oxidation process. However, this glassy protective layer can cause more severe cracks once the heating process is stopped and the temperature changes sharply, as observed in the experiment, shown in Fig. 5. The cooling rate was surprisingly high, with a decrease of almost 350°C within the first second once the ablation is stopped and an average rate of 85°C/s for the last 10 s, which induced thermal shock, resulting in further brittle cracks of the oxides layers (shown in Fig. 6).

3.2. Results and analysis for air/water vapor mix

The ablation test conditions and results of the specimens with water vapor are listed in Table 2. Compared with those in dry air, the average temperatures in Table 2 are about 20°C lower, since the water vapor changes the reflectivity of the specimen surface, and leads to temperature fluctuation of the infrared thermometer.

Table 2 shows that in the air/water vapor mix (5 wt%), the weight loss rates of the three types of specimens all decrease. The reason for this difference is that the humid air suppresses the melting and vaporization of the oxide product SiO_2 , thus more SiO_2 remains on the surface and prevents oxygen diffusing into the substrate.

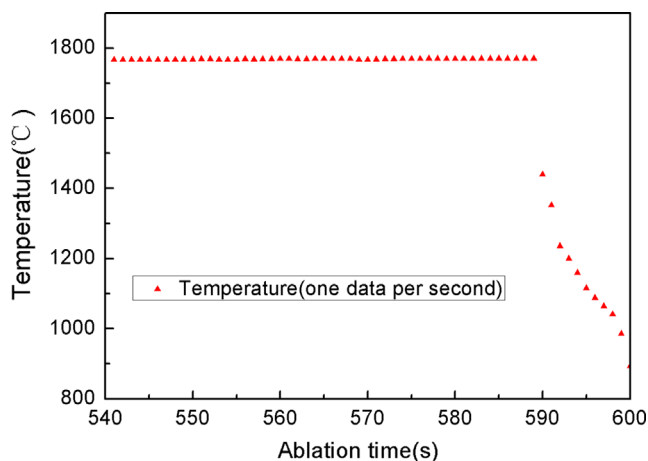
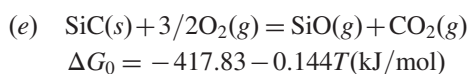
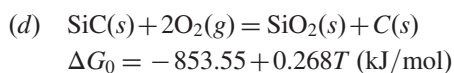
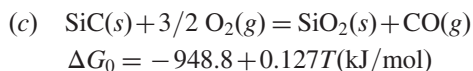
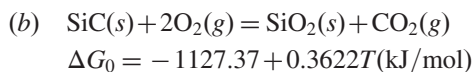
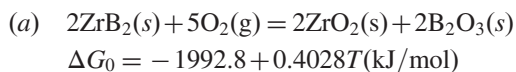


Fig. 5. Temperature decreases when ablation test is stopped.

As for the relatively higher weight loss rate of C/SiC-ZrO_2 and C/SiC-ZrB_2 , the reasons are explained below. For C/SiC-ZrB_2 , the possible reactions in the atmosphere of oxygen (for temperature range of $25\text{--}1700^\circ\text{C}$) are



Within the temperature range (around 1700°C) of the experiments in dry air, the main reactions of SiC-ZrB_2 will be (a) and (c) due to their lower ΔG_0 . The reaction in (a) generates B_2O_3 and ZrO_2 and the reaction in (c) produces SiO_2 . The melting point and boiling point of B_2O_3 is 445°C and 1500°C , respectively. Both are much lower than the ablation temperature. In addition, B_2O_3 has a strong ability to absorb water vapor and change into boric acid, which accelerates its volatilization. This leads to an increase of weight loss for C/SiC-ZrB_2 .

In addition, the morphologies of the air/water vapor mix specimens were examined with SEM as shown below in Figs. 7–9. It can be seen that in a wet atmosphere, the glassy SiO_2 and ZrO_2 generated are much less than in dry air: firstly, water vapor causes a decrease in viscosity and fluidity of the SiO_2 , thus no obvious “bone structures” were observed. In addition, the reaction between water vapor and B_2O_3 also

Table 2

Ablation test conditions and results of the specimens with water vapor.

Types	C/SiC	C/SiC–ZrO ₂	C/SiC–ZrB ₂
Weight loss rate (mg/s)	0.55	1.20	1.00
Ablation time (s)	600	600	600
Average temperature ($^\circ\text{C}$)	1740	1737	1729

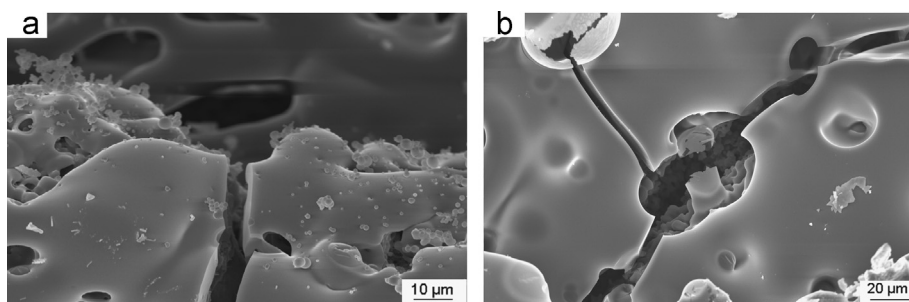


Fig. 6. Typical brittle cracks after the ablation (a) C/SiC-ZrO_2 and (b) C/SiC-ZrB_2 .

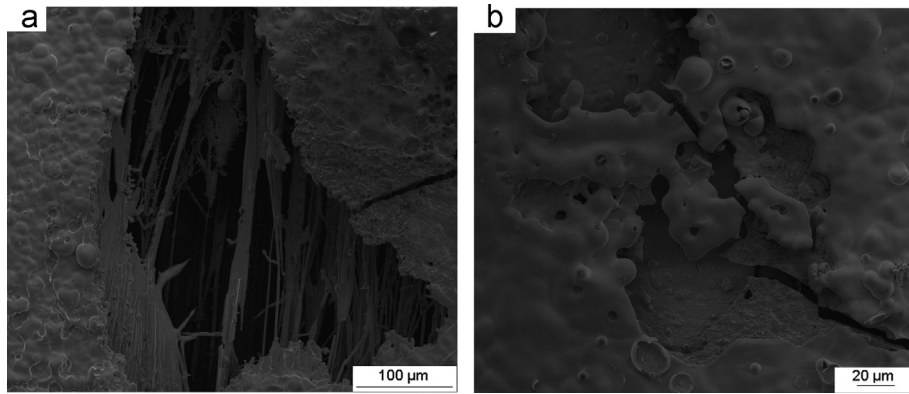


Fig. 7. Typical ablation morphologies of specimen C/SiC in air mixed with water vapor (a) center of ablation pit, and (b) edge of ablation pit.

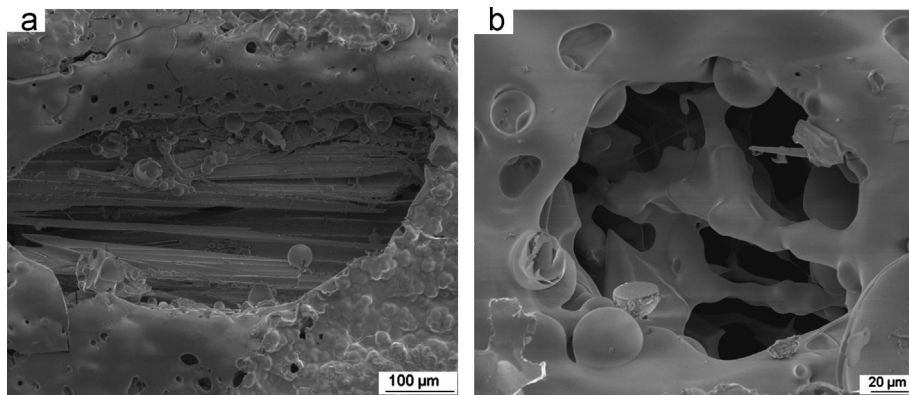


Fig. 8. Typical ablation morphologies of specimen C/SiC–ZrO₂ in air mixed with water vapor (a) center of ablation pit, and (b) edge of ablation pit.

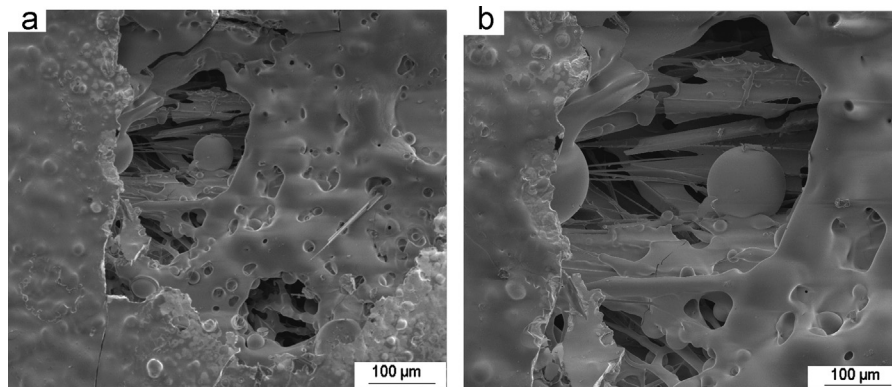


Fig. 9. Typical ablation morphologies of specimen C/SiC–ZrB₂ in mixed air with water vapor (a) center of ablation pit, and (b) edge of ablation pit.

reduced the quantity of boride. With water vapor, no obvious bubbling effect was observed during the ablation process.

3.3. Theoretical prediction of the weight loss of C/SiC composites

A model has been developed to predict the weight loss of the C/SiC composite. In this model, the weight loss of C/SiC composites is considered to be determined mainly by the competition between the generation and the loss of SiO₂. The rate of production of SiO₂ is calculated using the Arrhenius

equation, i.e. the reaction rate constant is

$$k = Ae^{-(E_A/RT)} \quad (1)$$

and it is assumed to be a diffusion-controlled process. The concentration of O₂ on the reaction surface is determined by the thickness of the SiO₂ already generated and the diffusion is calculated using Fick's first law. Thus the generation rate of SiO₂ is

$$\dot{m}_{\text{gain}} = k_1 Ae^{-(E_A/RT)} d_{\text{SiO}_2}^{-n} \quad (2)$$

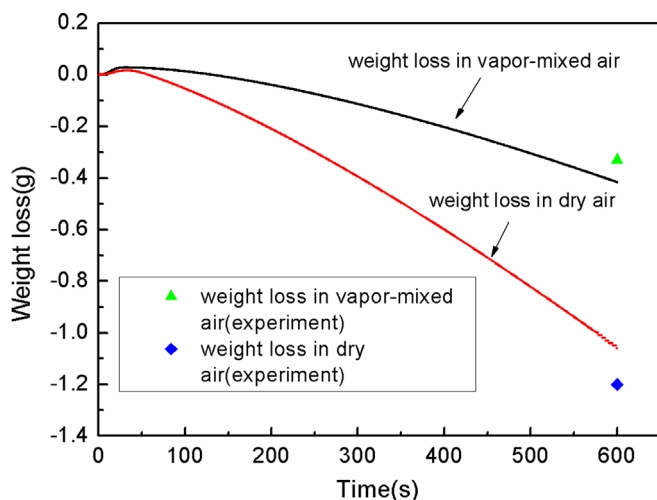


Fig. 10. Theoretical and experimental comparison of weight loss of C/SiC in dry air and mixed air with water vapor.

Furthermore, the weight loss rate of SiO_2 is assumed to be

$$\dot{m}_{\text{loss}} = \frac{k_2 d_{\text{SiO}_2}}{\mu} \quad (3)$$

where k_1 and k_2 are the reaction rate constants, A is a constant, E_A is the activation energy, R is the gas constant, T is the temperature, d_{SiO_2} is the thickness of SiO_2 , and μ is the coefficient of viscosity. And in Eq. (3) it is assumed that the loss rate of SiO_2 is related to the thickness and the coefficient of viscosity of SiO_2 .

Thus we have

$$\dot{m}_{\text{overall}} = \frac{k_1 A e^{-(E_A/RT)} d_{\text{SiO}_2}^{-n} - k_2 d_{\text{SiO}_2}}{\mu} \quad (4)$$

Based on Eq. (4), as at the beginning of the ablation, the thickness of SiO_2 is small, thus the overall weight increases first, and then with the accumulation of the SiO_2 and as d_{SiO_2} becomes bigger, the overall weight begins to decrease (i.e. weight loss), shown in Fig. 10. The two curves show good agreement with the experimental data.

4. Conclusions

The ablation behavior of C/SiC, C/SiC– ZrO_2 and C/SiC– ZrB_2 composites were investigated at 1700–1800 °C for 10 min via an oxyacetylene ablation test. Two different ablation conditions, dry air and air mixed with water vapor, were compared. Results show that in dry air the weight loss rate of C/SiC is the greatest, while the weight loss rate of C/SiC– ZrO_2 and C/SiC– ZrB_2 were almost the same. Furthermore, compared with the results in dry air, all weight loss rates decrease in wet air and the weight loss rate of C/SiC becomes the smallest. This work shows that in dry air, the C/SiC composite with additives ZrO_2 and ZrB_2 performs a much better thermal ablation resistance as well as in air mixed with water vapor, which is of great significance to further understand the working condition in combustion chambers. Future study will focus on the ablation test condition with inorganic

salts, to reveal the combined effect of salts and water vapor on the ablation properties of these composites.

Acknowledgments

We gratefully acknowledge the support from the National Natural Science Foundation of China (Grant nos. 90816007, 91116006, and 10902059), the Tsinghua University Initiative Scientific Research Program (No. 2011Z02173) and the Foundation for the Author of National Excellent Doctoral Dissertation of China (FANEDD) (No. 2007B30).

References

- [1] S. Schmidt, S. Beyer, H. Knabe, H. Immich, R. Meistring, A. Gessler, Advanced ceramic matrix composites materials for current and future propulsion technology applications, *Acta Astronaut.* 55 (3–9) (2004) 409–420.
- [2] G. Roewer, U. Herzog, K. Trommer, E. Muller, S. Fruhauf, Silicon carbide—a survey of synthetic approaches, properties and applications, in: M. Jansen (Ed.), *Structure and Bonding*, Vol. 101, High Performance Non-Oxide Ceramics I, Springer, Germany, Berlin, 2002, pp. 59–135.
- [3] H.O. Pierson, *Handbook of Refractory Carbides and Nitrides: Properties, Characteristics, Processing, and Applications*, Noyes Publications, Westwood, NJ, 1996.
- [4] T.M. Besmann, B.W. Sheldon, R.A. Lowden, D.P. Stinton, Vapor phase fabrication and properties of continuous filament ceramic composites, *Science* 253 (1991) 1104–1109.
- [5] R. Naslain, A. Guette, F. Rebillat, R. Pailler, F. Langlais, X. Bourrat, Boron-bearing species in ceramic matrix composites for long-term aerospace applications, *J. Solid State Chem.* 177 (2004) 449–456.
- [6] W. Krenkel, B. Heidenreich, R. Renz, C/C–SiC composites for advanced friction systems, *Adv. Eng. Mater.* 4 (2002) 427–436.
- [7] M.E. Westwood, J.D. Webster, R.J. Day, F.H. Hayes, R. Taylor, Oxidation protection for carbon fibre composites, *J. Mater. Sci.* 31 (6) (1996) 1389–1397.
- [8] Y.G. Wang, L.N. An, Y. Fan, L.G. Zhang, S. Burton, Z.H. Gan, Oxidation of polymer-derived SiAlCN ceramics, *J. Am. Ceram. Soc.* 88 (11) (2005) 3075–3080.
- [9] K. Upadhyaya, J.M. Yang, W.P. Hoffmann, Materials for ultrahigh temperature structural applications, *Am. Ceram. Soc. Bull.* 76 (12) (1997) 51–56.
- [10] Q.M. Liu, L.T. Zhang, J. Liu, X.G. Luan, L.F. Cheng, Y.G. Wang, The oxidation behavior of SiC–ZrC–SiC-coated C/SiC minicomposites at ultrahigh temperatures, *J. Am. Ceram. Soc.* 93 (12) (2010) 3990–3992.
- [11] E. Wuchina, M. Opeka, S. Causey, K. Buesking, J. Spain, A. Cull, J. Routbort, F. Guitierrez-Mora, Designing for Ultrahigh-temperature applications: the mechanical and thermal properties of HfB₂, HfCx, HfNx, and alpha Hf(N), *J. Mater. Sci.* 39 (19) (2004) 5939–5949.
- [12] Xufei Xuelin Dong, Xue Fang, Feng, Keh-Chih Hwang, Diffusion and stress coupling effect during oxidation at high temperature, *J. Am. Ceram. Soc.* 96 (1) (2013) 44–46.
- [13] A.K. Kuriakose, J.L. Margrave, The Oxidation kinetics of zirconium diboride and zirconium carbide at high temperatures, *J. Electrochem. Soc.* 111 (7) (1964) 827–831.
- [14] J.D. Bull, D.J. Rasky, C.C. Karika, Stability characterization of diboride composites under high velocity atmospheric flight conditions, in: *Proceedings of the 24th International SAMPE Technical Conference*, Toronto, Canada, 1992, pp. T1092–T1106.
- [15] F. Monteverde, The thermal stability in air of hot-pressed diboride matrix composites for uses at ultra-high-temperatures, *Corros. Sci.* 47 (8) (2005) 2020–2033.
- [16] A.L. Chamberlain, W.G. Fahrenholtz, G. Hilmas, D. Ellerby, Oxidation of ZrB_2 –SiC ceramics under atmospheric and re-entry conditions, *Refract. Appl. Trans.* 1 (2) (2005) 1–8.

- [17] A.L. Chamberlain, W.G. Fahrenholtz, G.E. Hilmas, D.T. Ellerby, Characterization of zirconium diboride for thermal protection systems, *Key Eng. Mater.* 264–268 (1) (2004) 493–496.
- [18] M.M. Opeka, I.G. Talmy, J.A. Zaykoski, Oxidation-based materials selection for 2000 °C hypersonic aero surfaces: theoretical considerations and historical experience, *J. Mater. Sci.* 39 (19) (2004) 5887–5904.
- [19] A.L. Chamberlain, W.G. Fahrenholtz, G.E. Hilmas, D.T. Ellerby, High strength zirconium diboride-based ceramics, *J. Am. Ceram. Soc.* 87 (6) (2004) 1170–1172.
- [20] F. Monteverde, A. Bellosi, Oxidation of ZrB_2 -based ceramics in dry air, *J. Electrochem. Soc.* 150 (11) (2003) B552–B559.
- [21] S.F. Tang, J.Y. Deng, S.J. Wang, W.C. Liu, K. Yang, Ablation behaviors of ultra-high temperature ceramic composites, *Mater. Sci. Eng. A—struct. Mater. Prop. Microstruct. Process* 465 (1–2) (2007) 1–7.
- [22] Q. Zhou, S.M. Dong, X.Y. Zhang, Y.S. Ding, Z.R. Huang, D.L. Jiang, Synthesis of the fiber coating by FP-CVI process, *Key Eng. Mater.* 336–338 (2007) 1307–1309.
- [23] Z. Wang, S.M. Dong, X.Y. Zhang, H.J. Zhou, D.X. Wu, Q. Zhou, D.L. Jiang, Fabrication and properties of Cf/SiC–ZrC Composites, *J. Am. Ceram. Soc.* 91 (10) (2008) 3434–3436.
- [24] Q.G. Li, S.M. Dong, Z. Wang, P. He, H.J. Zhou, J.S. Yang, B. Wu, J.B. Hu, Fabrication and properties of 3-D Cf/SiC–ZrC composites, using ZrC precursor and polycarbosilane, *J. Am. Ceram. Soc.* 95 (4) (2012) 1216–1219.
- [25] H.T. Wu, X. Wei, S.Q. Yu, W.G. Zhang, Ablation performances of multi-phased C/C–ZrC–SiC ultra-high temperature composites, *J. Inorg. Mater.* 26 (8) (2011) 852–856.
- [26] T.A. Parthasarathy, R.A. Rapp, M. Opeka, R.J. Kerans, A model for the oxidation of ZrB_2 , HfB_2 and TiB_2 , *Acta Mater.* 55 (17) (2007) 5999–6010.
- [27] L. Silvestroni, D. Sciti, C. Melandri, S. Guicciardi, Toughened ZrB_2 -based ceramics through SiC whisker or SiC chopped fiber additions, *J. Eur. Ceram. Soc.* 30 (11) (2010) 2155–2164.
- [28] W.G. Fahrenholtz, G.E. Hilmas, A.L. Chamberlain, J.W. Zimmermann, Processing and characterization of ZrB_2 -based ultra-high temperature monolithic and fibrous monolithic ceramics, *J. Mater. Sci.* 39 (2004) 5951–5957.
- [29] A. Rezaie, W.G. Fahrenholtz, G.E. Hilmas, evolution of structure during the oxidation of zirconium diboride–silicon carbide in air up to 1500 °C, *J. Eur. Ceram. Soc.* 27 (2007) 2495–2501.